Liquid Crystals
Publication details, including instructions for authors and subscription information:
http://www.informaworld.com/smpp/title~content=t713926090

New ferroelectric liquid crystalline materials containing one and two lactate groups attached to the molecular core

M. Garić; A. Bubnov[a]; V. Novotná[a]; M. Kašpar[a]; V. Hamplová[a]; D. Ž. Obadović; M. Glogarová[a]
[a] Department of Physics, Faculty of Sciences, University of Novi Sad, Novi Sad, Serbia and Montenegro

To cite this Article Garić, M. , Bubnov, A. , Novotná, V. , Kašpar, M. , Hamplová, V. , Obadović, D. Ž. and Glogarová, M.(2005) 'New ferroelectric liquid crystalline materials containing one and two lactate groups attached to the molecular core', Liquid Crystals, 32: 5, 565 — 572

To link to this Article: DOI: 10.1080/02678290500075134

URL: http://dx.doi.org/10.1080/02678290500075134

Liquid Crystals, Vol. 32, No. 5, May 2005, 565–572

New ferroelectric liquid crystalline materials containing one and two lactate groups attached to the molecular core

M. GARIĆ, A. BUBNOV*†, V. NOVOTNÁ†, M. KAŠPAR†, V. HAMPLOVÁ†, D. Ž. OBADOVIĆ and M. GLOGAROVÁ†

Department of Physics, Faculty of Sciences, University of Novi Sad, Novi Sad, Serbia and Montenegro
†Institute of Physics, Academy of Sciences of the Czech Republic, Na Slovance 2, 182 21 Prague, Czech Republic

(*Received 27 October 2004; accepted 15 January 2005*)

Several new liquid crystalline materials containing one, two or three chiral centres and having one or two lactate groups in the molecular core have been synthesized. Most of the materials show the blue phase, chiral nematic phase, paraelectric smectic A phase and orthogonal hexatic smectic B phase; some possess the ferroelectric SmC* phase. A study of the mesomorphic properties has been performed using differential scanning calorimetry, optical microscopy and X-ray diffraction. The thickness of the smectic layers and the value of the average distance between the long axes of neighbouring molecules were determined. In the SmC* phase, the temperature dependence of spontaneous polarization, spontaneous tilt angle and helical pitch was measured. The influence of the number of lactate groups on mesogenic behaviour has been established.

1. Introduction

The type of group connecting the chiral part to the rigid core of a mesogenic molecule seems to be very important in determing the mesomorphic behaviour. Recently, the effects have been established of exchanging (in the *Y*-position) the ester linkage group [1, 2] for an ether linkage [3, 4] on the mesomorphic properties of lactic acid derivatives with the core structure:

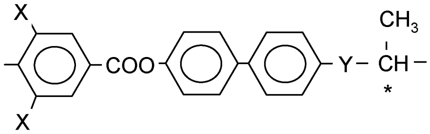

The incorporation of the ether linkage results typically in the disappearance of the SmC* phase [3].

The disappearance of the SmC* phase was also observed when exchanging the ester linkage group for an ether linkage in the *Y*-position for compounds with another type of the molecular core [5]:

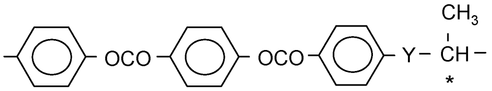

In materials having 2-octanol as a chiral chain, the exchange of the connecting group in the same position also led to a narrowing of an originally very broad SmC* phase, while the SmA phase remained [6, 7]. In that case a substantial decrease of the spontaneous polarization for the compounds with the ether linkage was observed [6]. It is suspected that the presence of the ether bond may disrupt the packing of the molecules in the SmC* phase layers.

The type of chiral fragment in the molecule is also very important in determing mesomorphic behaviour. Using a lactate-based chiral moiety has provided many materials with rather broad ferroelectric phases [3, 8–13]. Materials with two or more lactate units have been described in only a few cases [8, 14–16]; some of these showed the antiferroelectric phase.

These studies initiated a more detailed structural investigation using X-ray diffraction (XRD) on non-oriented samples [17]. From the XRD data we have determined some parameters of the phase structure: the layer spacing in the smectic (SmC*, SmA and SmB) phases, or the distance between the long molecular axes in the case of the blue phase (BP) and cholesteric (N*) phase, and the average intermolecular distance between the long axes of neighbouring parallel molecules.

The aim of this work was to establish the influence of the nature of the chiral chain and its total length on the formation of mesophases. Moreover, a comparison of the properties of compounds having one or two lactate units in the chiral part of the molecule has been

---

*Corresponding author. Email: bubnov@fzu.cz

Liquid Crystals
ISSN 0267-8292 print/ISSN 1366-5855 online © 2005 Taylor & Francis Group Ltd
http://www.tandf.co.uk/journals
DOI: 10.1080/02678290500075134

undertaken. The general chemical formulae of the materials studied are shown in table 1.

2. Synthesis

The synthesis of the compounds with one lactate group has been described elsewhere [3]. Here, the properties of new compounds from this series are presented. The general procedure for the preparation of the materials with two lactate units studied here is summarized in the scheme. All chiral centres are in the (*S*) configuration.

The mesogenic phenols (**1**) were obtained according to the scheme presented in [1]. The synthesis of the chiral units with two lactate groups has been described recently [8]. For the preparation of the final products, 0.02 mol of 4–(4′–hydroxybiphenyl) 4–alkoxybenzoate (**1**), 0.02 mol of chiral alcohol (**2a** or **2b**), and (11.0 g, 0.042 mol) of triphenylphosphine were dissolved in 100 ml of dried tetrahydrofuran and (7.4 g, 0.042 mol) of diethylazodicarboxylate was added drop wise. The reaction mixture was stirred overnight and the solvent removed under vacuum. The residue was dissolved in ethyl acetate and triphenylphosphine oxide precipitated by the addition of petroleum ether and filtered off. The filtrate was evaporated and the crude product chromatographed on Keiselgel 60 using dichloromethane ethanol (99/1) mixture. After crystallization from ethanol the product purity was determined by high pressure liquid chromatography using an HPLC chromatograph Ecom and a silica gel column Separon 7 µm, 3 × 150, Tessek with a toluene/methanol (99.9/0.1) mixture as eluent. The eluting products were detected by a UV-Vis detector (λ=290 nm). The chemical purity (determined by this method) of all the synthesized compounds was between 99.5% and 99.9%. The optical purity of all the studied compounds was higher than 96.0% with no racemization observed during synthesis.

Table 1. General formula of the liquid crystalline materials studied, with one or two lactate units. (*n* is the number of carbon atoms in the non-chiral chain; *x* is the number of the lactate groups; *R* denotes the type of the chiral chain).

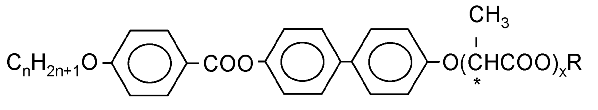

Compound	*n*	*x*	*R*
HOL 10/**	10	1	$CH_2C^*H(CH_3)CH_2CH_3$
HOL 12/6	12	1	C_6H_{13}
HOL 10/10	10	1	$C_{10}H_{21}$
HOLL 12/3	12	2	C_3H_7
HOLL 10/**	10	2	$CH_2C^*H(CH_3)CH_2CH_3$
HOLL 12/6	12	2	C_6H_{13}
HOLL 10/10	10	2	$C_{10}H_{21}$

The structures of the intermediates and final products were characterized by ^1H NMR spectroscopy using a 200 MHz Varian NMR spectrometer and solutions in $CDCl_3$, with tetramethylsilane as an internal standard.

^1H NMR (200 MHz, $CDCl_3$) for the mesogenic phenol/*n*=10/(**1**): 8.16 d (2H, *ortho* to –COO); 7.43 and 7.55 dd (4H, *ortho* to –Ar); 7.23 d (2H, *ortho* to –OCO); 6.99 d (4H, *ortho* to *R*O –); 6.78 d (2H, *ortho* to –OH); 5.00 brs. (1H, OH); 4.05 t (2H, CH_2OAr); 1.20–1.80 m (16H, CH_2); 0.90 t (3H, CH_3).

^1H NMR (200 MHz, $CDCl_3$) for the mesogenic phenol/*m*=12/(**1**): 8.16 d (2H, *ortho* to –COO); 7.43 and 7.55 dd (4H, *ortho* to –Ar); 7.23 d (2H, *ortho* to –OCO); 6.99 d (4H, *ortho* to *R*O –); 6.78 d (2H, *ortho* to –OH); 5.00 brs. (1H, OH); 4.05 t (2H, CH_2OAr); 1.20–1.80 m (20H, CH_2); 0.90 t (3H, CH_3).

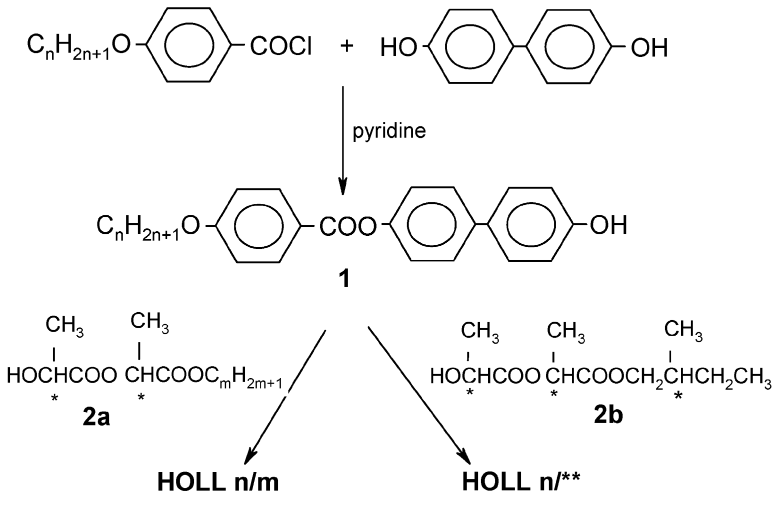

Scheme. General procedure for the synthesis of HOLL homologues.

^{1}H NMR (200 MHz, $CDCl_3$) for compound HOL 12/6: 8.18 d (2H, *ortho* to –COO); 7.55–7.62 (4H, *ortho* to –Ar); 7.26 d (2H, *ortho* to –OCO); 9.45 m (4H, *ortho* to –O*R*); 4.80 q (1H, Ar O $\underline{C^*H}$); 4.15 t (2H, COO$\underline{CH_2}$); 4.05 t (2H, CH_2OAr); 1.60 d (3H, $\underline{CH_3}$–C*); 1.20–1.90 m (28H, CH_2); 0.90 m (6H, CH_3).

^{1}H NMR (200 MHz, $CDCl_3$) for compound HOLL 12/6: 8.18 d (2H, *ortho* to –COO); 7.50–7.60 m (4H, *ortho* to –Ar); 7.25 d (2H, *ortho* to –OCO); 7.00 m (4H, *ortho* to –OR); 5.10 q (1H, Ar O $\underline{C^*H}$); 4.88 q (1H, COO$\underline{C^*H}$); 4.15 t (2H, COO$\underline{CH_2}$); 4.05 t (2H, CH_2OAr); 1.70 and 1.50 d+d (3H+3H, CH_3–C*); 1.20–1.90 m (28H, CH_2); 0.90 m (6H, CH_3).

3. Experimental results

Microscopic observations and measurements of the spontaneous quantities were performed on planar samples (in the bookshelf geometry) filled in the isotropic phase into 25 μm thick glass cells by means of capillary action. The inner surfaces of the glass plates were covered by ITO electrodes and polyimide layers unidirectionaly rubbed, to ensure planar geometry. Further improvement of the alignment, in order to obtain homogeneous texture, has been obtained using an electric field (10–20 Hz, 40 kV cm^{-1}) applied for 5–30 min. XRD studies were performed on non-oriented samples. Differential scanning calorimetry (DSC) was carried out on 3–6 mg samples placed in a nitrogen atmosphere and hermetically sealed in aluminium pans.

3.1. *Mesomorphic properties*

For all the materials synthesized, the sequence of phases and phase transition temperatures were determined on cooling from the isotropic phase using characteristic textures, and their changes observed on planar cells in polarizing optical microscopy (POM) (Nicon ECLIPSE E600POL). A Linkam LTS E350 heating stage with TMS 93 temperature programmer was used for temperature control ($\pm$0.1 K). The phase transition temperatures were checked by DSC using a Pyris Diamond Perkin-Elmer 7 on cooling and heating runs at a rate of 5 K min^{-1}. Typical examples of thermograms are presented in figure 1. Phase transition temperatures established from texture changes observed using POM during cooling are in good agreement with the positions of DSC peaks. The sequence of phases, melting points, phase transition temperatures and transition enthalpies for all the materials studied are listed in table 2.

All the compounds studied exhibit the blue phase, the cholesteric phase and the paraelectric SmA phase. The hexatic SmB phase occurs in the compounds with one lactate group and for one compound with two lactate groups and a long chiral chain. Only three compounds with a short chiral chain exhibit the ferroelectric SmC* phase. For compound HOL 12/6, a photomicrograph of the platelet texture of the blue phase is shown in figure 2. Such a texture is characteristic of the cubic blue phases, and probably corresponds to the BPII [18].

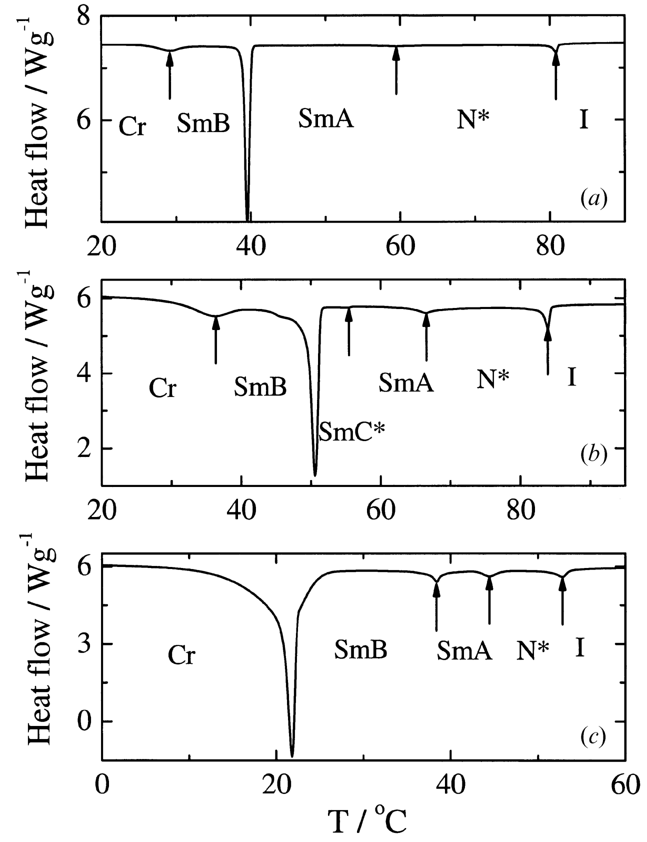

Figure 1. DSC traces for the compounds studied on cooling (*a*) HOL 10/10; (*b*) HOL 10/**, (*c*) HOLL 10/10. Arrows indicate the phase transition.

3.2. *Spontaneous quantities*

In the ferroelectric SmC* phase the temperature dependence of the spontaneous polarization $\mathbf{P}_s$, the spontaneous tilt angle θ_s of molecules from the smectic layer normal, and the helix pitch length p were measured. Values of the spontaneous polarization were evaluated from the **P**(**E**) hysteresis loop detected during $\mathbf{P}_s$ switching in an a.c. electric field **E** of frequency 60 Hz. Values of the spontaneous tilt angle were determined optically from the difference between extinction positions at crossed polarizers under opposite

Table 2. Sequence of phases, melting points m.p. (°C), phase transition temperatures (°C) and phase transition enthalpies ΔH (J g^{-1}), in brackets, measured on cooling (5 K min^{-1}) by DSC for the homologous series studied: 'msc' to indicates phase transition temperatures determined by microscope observations only.

Compound	m.p.	Cr		SmB		SmC*		SmA		N*		BP		I
HOL 10/**	54 (7.1)	•	36 (−3.2)	•	51 (−11.8)	•	55 (−0.1)	•	67 (−1.1)	•	84 (−1.3)	•	87 msc	•
HOL 12/6	51 (50.9)	•	28 (−0.1)	•	36 (−44.7)	•	61 (−0.1)	•	71 (−1.2)	•	91 (−1.2)	•	93 msc	•
HOL 10/10	48 (74.1)	•	29 (−2.8)	•	40 (−19.3)	—		•	60 (−0.8)	•	81 (−2.2)	•	83 msc	•
HOLL 12/3	52 (35.9)	•	30 (−1.4)	—		•	43 (−6.1)	•	64 (−1.2)	•	78 (−1.8)	•	79 msc	•
HOLL 10/**	45 (54.9)	•	31 (−9.7)	—		—		•	57 (−0.1)	•	64 (−1.1)	•	65 msc	•
HOLL 12/6	47 (50.3)	•	27 (−41.9)	—		—		•	42 (−0.6)	•	55 (−0.9)	•	56 msc	•
HOLL 10/10	65 (58.8)	•	23 (−28.1)	•	38 (−0.8)	—		•	45 (−1.1)	•	53 (−1.1)	•	54 msc	•

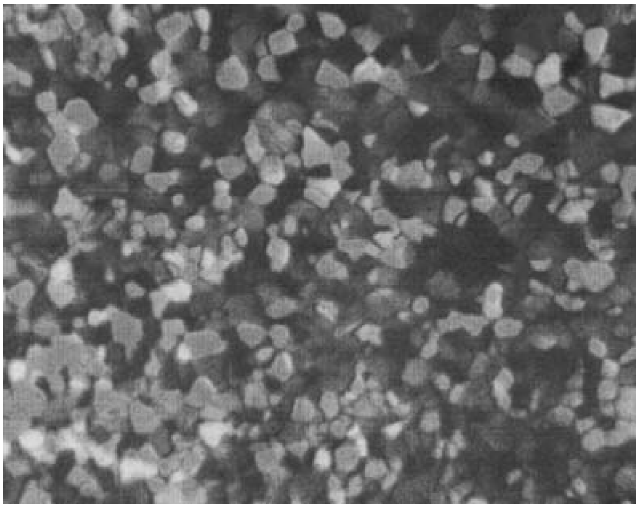

Figure 2. Microphotograph of the blue phase platelet texture between crossed polarizers for the compound HOL 12/6 taken at 91.5°C. The width of the photo about 150 µm.

d.c. electric fields of ±40 kV cm^{-1}. Well aligned samples were used for θ_s measurements.

For three materials possessing the ferroelectric SmC* phase, the temperature dependences of spontaneous polarization and spontaneous tilt angle are shown in figure 3. For the compounds studied the values of spontaneous tilt angle are about 21°–28° at saturation. The spontaneous polarization exhibits no saturation (see figure 3). For these compounds a linear $\mathbf{P}_s(\theta_s)$ relationship does not hold. Similar behaviour has been observed for materials based on lactic acid and having different chemical structures [13, 16, 19–22]. In the case of lactic acid derivatives, the competition between different conformers can be considered. It has been shown [23], that the continuous increase in $\mathbf{P}_s$ can

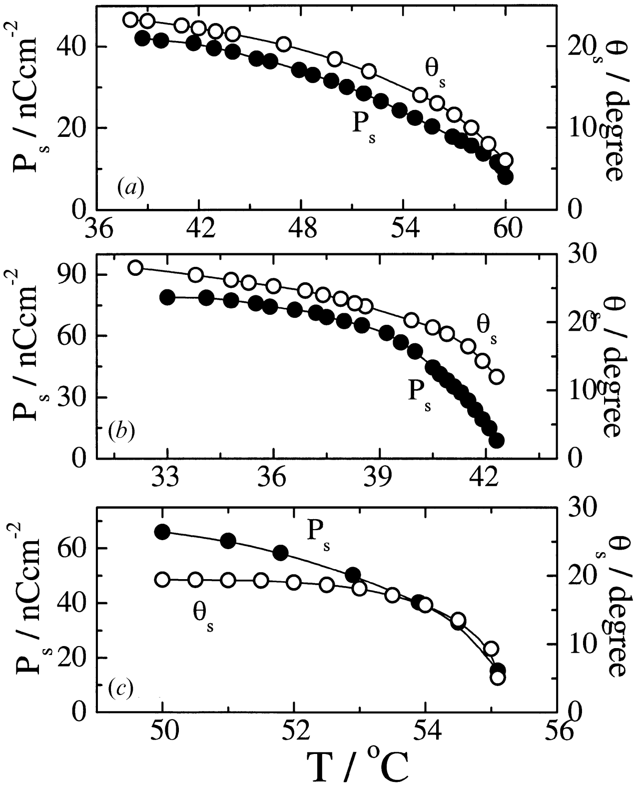

Figure 3. Temperature dependence of the spontaneous polarization ($\mathbf{P}_s$) and the spontaneous tilt angle (θ_s) for: (*a*) HOL 12/6, (*b*) HOLL 12/3, (*c*) HOL 10/**.

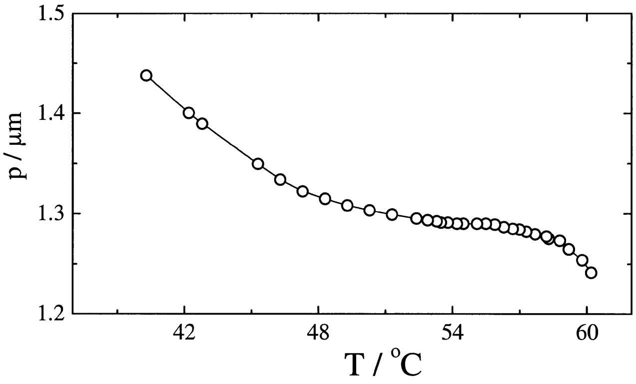

Figure 4. Temperature dependence of the helix pitch length for HOL 12/6.

be explained by the increase in concentration of conformers with a higher transversal dipole moment.

The values of the helix pitch length p were established by diffraction of He-Ne laser light (631 nm) on disclination lines, which exist in planar samples due to strong polar anchoring at the surfaces (dechiralization lines). The line spacing equals p. For compound HOL 12/6, temperature dependence of the helical pitch length in the SmC* phase is shown in figure 4. There is a slight increase of p on cooling just below the SmA phase, followed by a saturation, then a gradual increase. At the lower temperature border of the SmC* phase the helical pitch could not be measured as the spacing between dechiralization lines became rather high and irregular. It was impossible to measure the helix pitch length by the diffraction method for compounds HOLL 12/3 and HOL 10/**, as the spacing between the dechiralization lines was high and irregular over the whole temperature range of the ferroelectric SmC* phase.

3.3. *X-ray studies*

All the compounds were studied using XRD [17]. Non-oriented samples were studied in a transmission geometry using a conventional powder diffractometer, Philips PW 1350, with CuK_α radiation at 0.154 nm and a Ni filter. Diffractograms of all the compounds investigated were recorded in the diffraction angle range $2\theta=2°–35°$. An automated high temperature supplement HTK-10 (Paar) with the chamber connected to a vacuum pump was used. The samples were deposited on a platinum measuring plate connected to a Pt–10% RhPt thermocouple. Sample temperature variation was regulated by temperature controller HTK2-HC (Paar) and the heating/cooling rate was 1 K min^{-1}.

The layer spacing d and the average repeat distance D between the long axes of neighbouring parallel molecules were determined using Bragg's law: $n\lambda=2d\sin\theta$. The values of d and D were calculated from the position of the small angle and wide angle diffraction peaks, respectively. In the hexatic SmB phase, the intermolecular distance b between the long axes of neighbouring parallel molecules can be calculated as $b=2D/3^{1/2}$[24].

In figure 5, examples of the XRD profiles obtained on the non-oriented samples as a function of temperature are presented for all the phases studied. Analysis of the X-ray diagrams shows the presence of reflections at small angles ($2\theta\sim3°–4°$), indicating the layer structure, as well as diffuse outer scattering ($2\theta\sim18.5°–24°$) corresponding to the average intermolecular distance D. The results of the X-ray studies for the HOL series are collected in table 3 and for the HOLL series in table 4.

The temperature dependence of the layer spacing for HOL 10/**, HOL 10/10 and HOLL 10/10 is shown in figure 6. It is rather unusual that the layer spacing values in the SmB phase are smaller than those in the higher temperature smectic phases. This may be explained by partial overlapping of the chain ends, which occurs due to hydrogen bonding between the chains.

In the case of the blue phase and the cholesteric phase, the small angle peak ($2\theta\sim3°–4°$), corresponding to long spacing distance, is approximately equal to the length of the molecule. At the SmC*→SmB phase transition an increase of intensity in the small angle reflection ($2\theta\sim3.9°$) is detected, corresponding to an increase of the orientation order of the long molecular axes. In addition, a strong peak at $2\theta\sim20°$ is present in the SmB phase (see figure 5); this peak corresponds to the hexagonal molecular packing of the centres of mass of the molecules within the smectic layers and characterizes the hexatic SmB phase.

The experimental results show that in the SmB phase, the compounds with one lactate group exhibit a larger layer spacing than those with two lactate groups and the same length of the molecular chains. The most significant difference in the layer spacing values is found for compounds HOL 10/10 and HOLL 10/10, whose layer spacings are about 26 Å, and 24.5 Å, respectively (see tables 3 and 4 and figure 6). This may be explained by the effect of the additional lactate group which acts against the extension of the chiral chain. Similar behaviour was observed for liquid crystalline materials differing in the number of the lactate groups [15]: the effective layer spacing d/L

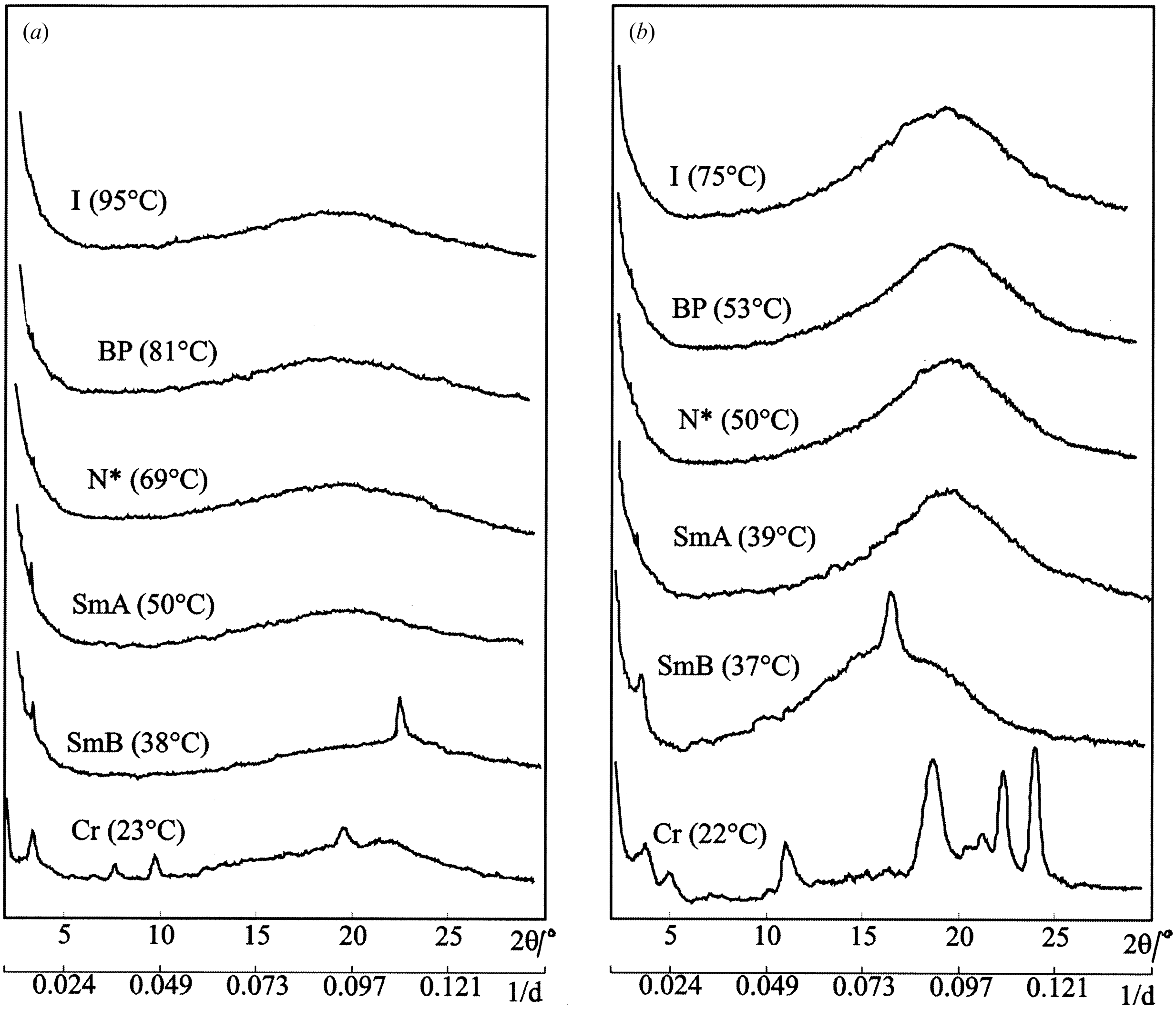

Figure 5. X-ray diffraction profiles for (*a*) HOL 10/10 and (*b*) HOLL 10/10.

decreases with increase of the lactate group number (*L* is the calculated length of the molecule).

4. Discussion and conclusions

Two new series of chiral liquid crystalline materials, differing in the number of (*S*)-lactate groups in the chiral part of the molecule, have been synthesized and characterized. All the compounds show the blue phase, the cholesteric phase and the paraelectric SmA phase. In the HOL series, only compounds having the shortest chiral chain show the ferroelectric SmC* phase.

A decrease in phase transition temperature is observed on increasing the number of lactate groups from 1 to 2, as for materials with the keto group attached to the molecular core [15] instead of the oxygen used here, and also for materials with an *n*-butyl chain [8, 16] instead of the (*S*)-2-methylbutyl moiety in the chiral segment.

The results of the study show that the spontaneous polarization increases and the spontaneous tilt angle decreases on increasing the number of chiral centres.

X-ray data show that the intermolecular distance between the long axes of neighbouring parallel molecules decreases on cooling from the isotropic phase to the orthogonal smectic B phase. This indicates an increase of the molecular packing density.

It is rather unusual that the layer spacing values in the SmB phase are smaller than those in the higher temperature smectic phases. This may be explained by partial overlapping of the molecular chain ends, which occurs due to hydrogen bonding between the molecular chains.

Table 3. Molecular parameters of the HOL series in all phases observed at a fixed temperature *T*: effective layer thickness *d* (error of measurements δ_d was about ± 0.05 Å), average distance between long molecular axes *D* (error of measurements δ_D was about ± 0.002 Å) and intermolecular distance *b* in the SmB phase. In the BP and N* phases, *d* equals approximately the length of the molecule.

Compound	Phase	*T*/°C	*d*/Å	*D*/Å	*b*/Å
HOL 10/**	I	110	—	4.689	—
	BP	86	27.58	4.665	—
	N*	74	26.34	4.689	—
	SmA	59	25.21	4.524	—
	SmC*	53	24.86	4.547	—
	SmB	40	24.18	4.434	5.120
HOL 12/6	I	100	—	4.739	—
	BP	92	29.42	4.689	—
	N*	80	—	4.593	—
	SmA	68	23.22	4.524	—
	SmC*	50	22.06	4.501	—
	SmB	33	22.62	4.423	5.107
HOL 10/10	I	95	—	4.595	—
	BP	82	27.58	4.570	—
	N*	69	26.74	4.665	—
	SmA	50	27.58	4.605	—
	SmB	38	25.96	3.947	4.558

Table 4. Molecular parameters of the HOLL series in all phases observed at a fixed temperature *T*: key as for table 3.

Compound	Phase	T/°C	d/Å	D/Å	b/Å
HOLL 12/3	I	85	—	4.689	—
	BP	78	23.85	4.665	—
	N*	70	—	4.642	—
	SmA	56	23.85	4.605	—
	SmC*	40	22.63	4.547	—
HOLL 10/**	I	77	—	4.689	—
	BP	64	24.86	4.524	—
	N*	60	23.85	4.570	—
	SmA	50	23.85	4.547	—
HOLL 10/10	I	75	—	4.665	—
	BP	53	29.42	4.524	—
	N*	50	29.42	4.570	—
	SmA	40	28.52	4.547	—
	SmB	37	24.51	3.629	4.190

Acknowledgements

This work was supported by: Grants No. 202/03/P011, 202/02/0840, 202/05/0431 from the Grant Agency of the Czech Republic, Grant No. 1578 from the Ministry of Science, Technologies and Development of the Republic of Serbia; Research Project AVOZ1−010−914, and European Project COST D14 WG15.

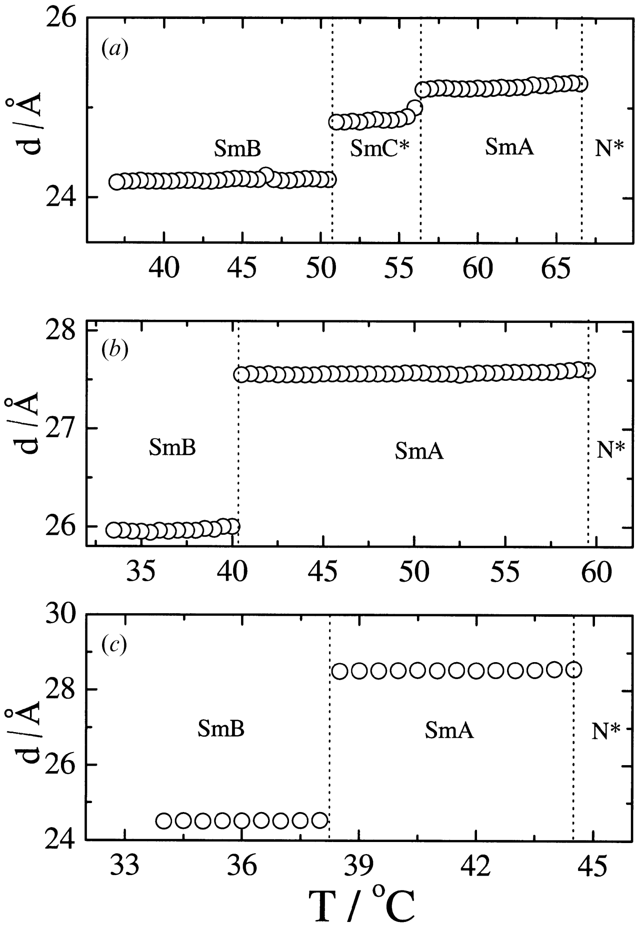

Figure 6. Temperature dependence of the layer spacing *d* for: (*a*) HOL 10/**, (*b*) HOL 10/10, (*c*) HOLL 10/10.

References

[1] M. Kašpar, M. Glogarová, V. Hamplová, H. Sverenyák, S.A. Pakhomov. *Ferroelectrics*, **148**, 103 (1993).

[2] A. Vajda, M. Kašpar, V. Hamplová, S.A. Pakhomov, P. Vaněk, K. Fodor-Csorba, L. Bata. *Mol. Cryst. liq. Cryst.*, **351**, 279 (2000).

[3] A. Bubnov, S.A. Pakhomov, M. Kašpar, V. Hamplová, M. Glogarová. *Mol. Cryst. liq. Cryst.*, **328**, 317 (1999).

[4] A. Vajda, V. Hamplová, M. Kašpar, A. Bubnov, D.Ž. Obadović, N. Eber, K. Fodor-Csorba. *J. Res. Phy.*, **29**, 107 (2003).

[5] Unpublished results of Prague group — EO- and QO-series.

[6] A. Yoschizawa, I. Nishiyama, M. Fukumasa, T. Hirai, M. Yamane. *Jpn. J. appl. Phys.*, **28**, L 1269 (1989).

[7] T. Inukai, S. Saiton, H. Inoue, K. Miyazawa, K. Terashima, K. Furukawa. *Mol. Cryst. liq. Cryst.*, **141**, 251 (1986).

[8] M. Kašpar, V. Hamplová, V. Novotná, M. Glogarová, D. Pociecha, P. Vaněk. *Liq. Cryst.*, **28**, 1203 (2001).

[9] W.-L. Tsai, T.-C. Lu, H.-W. Liu, M.-Y. Tsai, C.-M. Fu. *Liq. Cryst.*, **27**, 1389 (2000).

[10] H. Taniguchi, M. Ozaki, K. Yoshino, K. Satoh, N. Yamasaki. *Ferroelectrics*, **77**, 137 (1988).

[11] W.-L. Tsai, S.-W. Yen, M.-J. Hsie, H.-C. Lee, C.-M. Fu. *Liq. Cryst.*, **29**, 251 (2002).

[12] J. Matsushima, Y. Takanishi, K. Ishikawa, H. Takezoe, A. Fukuda, C.S. Park, W.-G. Jang, K.-H. Kim, J.-E. Maclennan, M.A. Glaser, N.A. Clark, K. Takanishi. *Liq. Cryst.*, **29**, 27 (2002).

[13] V. Hamplová, A. Bubnov, M. Kašpar, V. Novotná, M. Glogarová. *Liq. Cryst.*, **30**, 493 (2003).

[14] S. Mery, D. Lottzsch, G. Heppke, R. Shashidhar. *Liq. Cryst.*, **23**, 629 (1997).

[15] V. Hamplová, A. Bubnov, M. Kašpar, V. Novotná, D. Pociecha, M. Glogarová. *Liq. Cryst.*, **30**, 627 (2003).

[16] V. Hamplová, A. Bubnov, M. Kašpar, V. Novotná, Y. Lhotáková, M. Glogarová. *Liq. Cryst.*, **30**, 1463 (2003).

[17] D.Ž. Obadović, L. Bata, T. Thot-Katona, A. Bota, K. Fodor-Csorba, A. Vajda, M. Stančić. *Mol. Cryst. liq. Cryst.*, **303**, 85 (1997).

[18] I. Dierking. *Textures of Liquid Crystals*, p. 218, Wiley-VCH, Weinheim (2003).

[19] V. Novotná, M. Kašpar, V. Hamplová, M. Glogarová. *Liq. Cryst.*, **29**, 1435 (2002).

[20] M. Kašpar, V. Hamplová, S.A. Pakhomov, A.M. Bubnov, F. Guittard, H. Sverenyák, I. Stibor, P. Vaněk, M. Glogarová. *Liq. Cryst.*, **24**, 599 (1998).

[21] S.L. Wu, C.Y. Lin. *Liq. Cryst.*, **29**, 1575 (2002).

[22] S.L. Wu, C.Y. Lin. *Liq. Cryst.*, **30**, 471 (2003).

[23] E. Gorecka, M. Glogarová, H. Sverenyák, M. Kašpar, V. Hamplová, S.A. Pakhomov. *Ferroelectrics*, **179**, 81 (1996).

[24] J.M. Seddon. *Handbook of Liquid Crystals*, Vol. 1, D. Demus, J. Goodby, G.W. Gray, H.-W. Spiess, V. Vill (Eds), p. 635, Wiley-VCH, Weinheim (1998).